DOI: https://doi.org/10.14256/JCE.4320.2025

Primljen / Received: 7.5.2025.
Ispravljen / Corrected: 6.8.2025.
Prihvaćen / Accepted: 29.9.2025.
Dostupno online / Available online: 10.2.2026.

Experimental investigation of sustainable gamma radiation shielding concrete

Authors:

Assoc.Prof. **Vadivel Murugesan**, PhD. CE
Nehru Institute of Technology, Coimbatore, India
Department of Civil Engineering
vadivelnitcbe@gmail.com
Corresponding author

Assoc.Prof. **Senthil Kumar Govindan**, PhD. CE
SRM Easwari College of Engineering, Chennai, India
Department of Civil Engineering
govindsenthilme@gmail.com

Assoc.Prof. **Natarajan Seralathan**, PhD. CE
Madha College of Engineering, Chennai, India
Department of Civil Engineering
sera.natraj1@gmail.com

Amirtharaj John, MCE
Anna University, Chennai, India
Department of Civil Engineering
amirthavijay1@gmail.com

Research Paper

Vadivel Murugesan, Senthil Kumar Govindan, Natarajan Seralathan, Amirtharaj John

Experimental investigation of sustainable gamma radiation shielding concrete

The construction industry is increasingly adopting sustainable practices to mitigate the environmental impact from excessive consumption of natural aggregates. This study investigated the incorporation of copper slag (CS) and recycled ceramic tiles (RCT) as partial aggregate replacements in concrete at levels ranging from 50 % to 90 %, with a focus on both the structural integrity and gamma radiation shielding performance. Results indicated improvements in slump, density, and compressive, tensile, and flexural strengths. The optimal mixture, with 60 % replacement, exhibited a maximum density increase increases of 45.9 % and an 18.18 % enhancement in attenuation coefficient (μ). A strong correlation (R^2 = 0.9743) between density and μ confirms the effectiveness of these materials, making CS and RCT viable sustainable aggregate alternatives for radiation shielding concrete.

Key words:
sustainable concrete, copper slag, recycled tiles, mechanical properties, radiation shielding

Prethodno priopćenje

Vadivel Murugesan, Senthil Kumar Govindan, Natarajan Seralathan, Amirtharaj John

Eksperimentalno ispitivanje održivog betona za zaštitu od gama-zračenja

U građevinskom se sektoru sve intenzivnije primjenjuju održiva rješenja kako bi se umanjio negativan utjecaj prekomjerne potrošnje prirodnih agregata na okoliš. U ovom je istraživanju ispitano uključivanje bakrene zgure (CS) i recikliranih keramičkih pločica (RCT) kao djelomične zamjene agregata u betonu, u udjelima od 50 % do 90 %, s težištem na mehaničkim svojstvima i sposobnosti zaštite od gama-zračenja. Utvrđena su poboljšanja u obradljivosti svježeg betona, gustoći, tlačnoj i vlačnoj čvstoći te čvrstoći na savijanje. Optimalna smjesa, sa 60-postotnom zamjenom, ostvarila je porast gustoće od 45,9 % te poboljšanje koeficijenta prigušenja (μ) od 18,18 %. Jaka korelacija (R^2 = 0,9743) između gustoće i koeficijenta μ potvrđuje učinkovitost tih materijala, pri čemu su se CS i RCT pokazali kao održiva i dostojna zamjena agregata u betonu za zaštitu od zračenja.

Ključne riječi:
održivi beton, bakrena zgura, reciklirane pločice, mehanička svojstva, zaštita od zračenja

1. Introduction

Natural aggregates constitute approximately 60-80 % of the total concrete volume [1, 2]. Owing to the increasing scarcity of these materials, the construction industry has been actively investigating substitute materials, particularly as quarrying natural aggregates consumes significant water resources [3, 4]. The extraction and processing of these raw materials contribute to environmental degradation and climate change while demanding considerable electrical energy. Additionally, the supply of fine aggregates is restricted by seasonal and environmental conditions, including heavy rain and flooding [5]. River sand extraction, a primary source of fine aggregates, results in adverse ecological impacts such as erosion and depletion of natural resources. Therefore, exploring a sustainable, affordable, and consistently available alternative aggregate material has become crucial. A particularly effective approach involves the use of waste by-products in concrete as substitutes for natural aggregates. Numerous studies have examined the feasibility of incorporating recycled materials into concrete to enhance ductility and reduce weight [6]. Copper slag has emerged as a promising alternative owing to its comparable silica (SiO_2) content and physical characteristics to that of river sand. The copper slag is typically irregular, glassy, black, and granular. The production of one ton of copper generates 2.2 to 3 tons of copper slag [7]. These industries produce approximately 400,000 tons of Cu each year, yielding nearly 800,000 tons of copper slag each year. Earlier studies [7-10] demonstrated its capability to improve the mechanical performance of concrete when used as a fine aggregate, which confirmed the suitability of copper slag in concrete applications. Evidence from earlier studies [11-14] suggested that the partial substitution of fine aggregates with copper slag can significantly enhance the strength and durability of concrete. Similarly, reusing tile waste as an aggregate in concrete is particularly significant because it considerably reduces waste disposal and helps preserve natural aggregate resources. The 3rd generation of wall and floor ceramics represents the latest technology in the form of porcelain ceramics. Manufacturers produce porcelain, a uniform material, by forming granules under high pressure and firing them at high temperatures. The granule shape of and moisture content promote interlocking during compression, which enhance the structural strength of the porcelain. The final stage of the production process at 1400°C results in the formation of highly stable phases in the porcelain, enhancing its resistance to reactants and ensuring a stable condition. The final products are compact and appear white [15]. High annealing temperatures and low porosity enable porcelain ceramics to achieve high strength with a water absorption rate of less than 0.3 %. Porcelain production continues to increase as market demand increases. In recent years, ceramic tile manufacturing has expanded significantly, with global production increasing from 8,581 million square meters in 2009 to 16,093 million square meters in 2020. Within the European Union, Spain is the primary producer and ranks second globally. In 2020, the country exported 415 million square meters, representing 81.4 % of its total ceramic tile production [16]. Incorporating ceramic tile waste (CTW) into reuse practices supports circular economy goals by reducing the demand for natural raw materials and minimising the ecological footprint associated with landfilling. The primary sources of tile waste include the ceramic tile industry, remnants of newly constructed structures, and demolition debris from older buildings. The ceramic tile industry experiences considerable manufacturing losses, with approximately 7 % of produced tiles failing to meet quality standards, owing to size variation, glazing defects, and cracking during firing. Manufacturers seldom reuse or recycle these non-standard tiles during production [17]. These tile wastes are stored in specific waste dumps located close to their production facilities without sorting their contents. The storage of waste products has become a major environmental issue, particularly in areas where disposal sites are limited. Recycling waste porcelain ceramics and returning them to production lines is not feasible, leading to their unavoidable disposal into the environment. The reutilisation of waste tiles as aggregates in concrete is not novel in concrete technology, and numerous studies [18-22] have discussed this practice.

Various radiation sources and instruments are used in hospitals, research centres, petrochemical industries, refining industries, and nuclear power plants [23]. Gamma rays represent the most destructive type of radiation emitted from radioactive waste and nuclear explosions [24, 25]. Prolonged exposure to nuclear radiation leads to immune system dysregulation and cancer in humans, and high doses can lead to immediate death [26-28]. The fundamental principle of radiation shielding can be easily understood as follows: when a ray traverses an antiradiation material, a portion of the incident photon's energy is absorbed by the antiradiation material, causing the original photon to scatter, which alters its path and direction, thereby reducing the radiation energy. Materials with high densities and atomic numbers provide good radiation attenuation [29]. Typical gamma-ray shielding materials include tungsten, lead, iron, metal alloy, and heavy aggregates such as hematite, barite, and magnetite [30, 31]. Among these, lead is the most commonly used because it exhibits a high atomic number and density while providing an excellent photoelectric effect. Many hospitals and research centres utilize lead plates or lead sheets as their primary radiation barriers.

Concrete has serves as an effective radiation shielding material [32-34], and is often termed radiation shielding concrete (RSC). This specialised concrete is essential for protecting individuals from the detrimental effects of ionising radiation in high-risk settings such as nuclear power facilities, hospitals that use radiological equipment, and aerospace operations where radiation poses serious health hazards. This concrete helps reduce exposure to radiation, thereby preventing radiation sickness and various cancers and ensuring the personnel and public safety. Furthermore, RSC is instrumental in the safe handling and storage of radioactive materials in research and industrial sectors. The innovation and improvement of RSC are essential for enhancing protective measures and reducing radiation-related risks. Since its introduction in the mid-1900s, this material has undergone considerable advancements, largely driven by developments in nuclear technology and medical imaging. Traditionally, RSC is referred to as high-density concrete, which includes heavyweight aggregates such as magnetite, barite, and ilmenite to make high-density concrete for better radiation protection, resulting in effective attenuation of neutrons and photons [35, 36]. The density of heavyweight concrete primarily depends on the specific gravity of the concrete used. In general, concrete with a specific gravity higher than 2.6 is referred to as heavyweight concrete, whereas an aggregate with a specific gravity higher than 3 is referred to as heavyweight aggregate. González-Ortega et al. [37] incorporated barite powder and aggregate into heavy-weight concrete for nuclear facilities and hospital radiation shielding. Ouda and Abdel-Gawwad [38] analysed the physical, mechanical, and gamma-ray attenuation properties of heavyweight concrete made with magnetite, goethite, and barite aggregates. Cullu and Bakirhan [39] reported that the strength of concrete significantly influenced the radiation absorption coefficient of heavyweight lead-zinc concrete. Papachristoforou and Papayianni [40] developed a radiation-shielding concrete using electric-arc furnace (EAF) slag aggregates reinforced with steel fibres. They observed that the linear attenuation coefficients of the concrete measured for photon energies of 244, 344, 779, 964, 1112, and 1408 keV showed an increase of 10 to 15 % compared with conventional concrete, depending on the photon energy. These findings indicate that EAF slag and steel fibres can be utilised to produce an efficient and alternative RSC that meets higher strength requirements. Dezhampanah et al. [41] examined the impact of incorporating nano TiO_2 particles on the properties of concrete and observed that it improved the compressive strength by 15.5 %. For 8 % nano TiO_2 particles, the μ for photon energies of 1332, 1170, and 662 keV increased by 7.8 %, 5.4 %, and 8.9 % respectively. Similarly, Rawat et al. [42] investigated the effect of incorporating nano TiO_2 particles on the properties of concrete. Abo-El-Enein et al. [43] reported that the addition of 2 % haematite nanoparticles enhanced compressive strength by approximately 20 %. Furthermore, the linear attenuation coefficients improved by 6 %, 3 %, and 11 % at 3, 28, and 90 d, respectively. Waste materials have also been used in the development of RSC. These initiatives are in accordance with the sustainable development goals (SDGs) established by the United Nations (UN), which present a vision for sustainable development across various sectors. In particular, the primary objectives of the SDGs focus on waste management and circular economy. It encompasses sustainable consumption and production (SDG-12) and climate action (SDG-13). Ling and Poon [44] examined the potential application of recycled cathode ray-tube (CRT) funnel glass as an aggregate in concrete. They observed that the recycled CRT aggregate was used as an aggregate in concrete, resulting in a significant increase in the concrete density. However, they concluded that barite addition reduced the concrete compressive strength and splitting tensile strength, while causing a decline in the elastic modulus. Alwaeli [45] found that the incorporation of lead-zinc slag waste into concrete improved the compressive strength by 20 % and gamma attenuation by 23.1 %. Baalamurugan et al. [46] observed that the incorporation of furnace steel slag aggregates resulted in a 7 % increase in the compressive strength with improved shielding performance, increasing the gamma attenuation factor by 14.5 % and 5.8 %. Studies on the use of waste materials as aggregates for RSC are limited. Therefore, this study investigated the properties of gamma RSC incorporating copper slag and tile waste as aggregates.

2. Materials and methodology

2.1. Materials

The raw materials used in this study are shown in Figure 1. In this study, ordinary Portland cement (OPC) of 53 grade, from the Coromandel brand, served as the primary binder, complying with IS: 12269-1987 [47] specifications. Tables 1 and 2 list the chemical compositions and properties of the cement. M-sand was used as a fine aggregate in concrete, as per IS: 383-1970 [48] specifications. Table 3 lists the properties of M-sand. Well-graded angular granite stone with a particle size of 12.5 mm 20 mm was utilised as a coarse aggregate in the concrete. Table 4 lists the properties of the coarse aggregates. Portable tap water free from oils, salts, organic materials, and alkalis was used. The water had a pH of 7, meeting the IS: 456-2000 [49] standards. A high-range water-reducing chemical was used as the chemical admixture for the concrete mixture. A polycarboxylate-ether-based superplasticiser which fulfilled the requirements set by ASTM C 494-13 [50] was used at rate 0.5 % weight of cement. In this study, copper slag sourced from Sterlite Industries India Limited (SIIL) in Tuticorin was utilized. Prior studies [51-54]

Figure 1. Raw material for concrete production: a) cement; b) small aggregate; c) coarse aggregate; d) superplasticizer; e) copper slag; f) recycled ceramic tiles; g) water

Table 1. Chemical composition of cement and copper slag

Component	Cement [%]	Copper slag [%]
SiO_2	22.02	31.92
Fe_2O_3	5.12	59.11
Al_2O3	5.59	2.52
CaO	60.84	1.25
MgO	122	1.65
Na_2O	0.29	1.40
K_2O	0.67	0.81
SO_3	-	1.34

Table 2. Properties of cement

Properties	Values	Requirements as per IS: 12269-1987 [47]
Normal consistency	31 %	25 % - 35 %
Specific gravity	3.15	3.15
Setting time (initial)	40 minutes	Not less than 30 minutes
Setting time (final)	345 minutes	Ne više od 600 minutes
Fineness	330 m²/kg	Not less than 225 m²/kg
Soundness	2.50 mm	Less than 10 mm

Figure 2. Ceramic tile waste

Figure 3. Recycled Ceramic tiles (RCTs)

concluded that concrete or mortar incorporating copper slag at higher replacement levels as fine aggregate exhibited a strength higher than those of the control samples. Accordingly, copper slag was used as an alternative to fine aggregates (M-sand) at replacement levels of 50 %, 60 %, 70 %, 80 %, and 90 %. Table 3 lists the properties of the copper slag. The ceramic waste material used in this study comprised crushed porcelain tiles sourced from construction waste. Manual breaking and subsequent mechanical processing produced particles in the range of 4.75-12.5 mm for use as coarse aggregate, as illustrated in Figures 2 and 3. Table 4 outlines the properties of the recycled ceramic tiles. Recycled ceramic tiles were used as an alternative to coarse aggregate at replacement levels of 50 %, 60 %, 70 %, 80 %, and 90 %.

Table 3. Properties of the M-sand and copper slag

Properties	M-sand	Copper slag	IS Standards
Dry compacted bulk density [kg/m³]	1646	2150	IS: 2386 (Part 3) [55]
Loose compacted bulk density [kg/m³]	1532	1840	IS: 2386 (Part 3) [55]
Specific gravity	2.6	2.61	IS: 2386 (Part 3) [55]
Fineness modulus	2.75	3.17	IS: 2386 (Part 1) [56]
Moisture content [%]	4	0.01	IS: 2386 (Part 3) [55]

Table 4. Properties of the coarse aggregate and recycled ceramic tiles (RCT)

Properties	Coarse aggregate	Recycled Ceramic Tile (RCT)	IS Standards
Dry compacted bulk density [kg/m³]	1850	1700	IS: 2386 (Part 3) [55]
Loose compacted bulk density [kg/m³]	1600	1550	ISO: 2386 (Part 3) [55]
Specific gravity	2.65	2.45	IS: 2386 (Part 3) [55]
Fineness modulus	7.1	6.2	IS: 2386 (Part 1) [56]
Moisture content [%]	0.2	0.4	IS: 2386 (Part 3) [55]

Table 5. Mix proportion

Mix ID	Cement [kg/m³]	Fine aggregate [kg/m³]	Cooper slag (CS) [kg/m³]	Coarse aggregate [kg/m³]	Recycled ceramic tile (RCT) aggregate [kg/m³]	Water [kg/m³]	Superplasticizer [kg/m³]
CC	400	700	0	1050	0	180	2
RSC 1	400	350	350	525	525	180	2
RSC 2	400	280	420	420	630	180	2
RSC 3	400	210	490	315	735	180	2
RSC 4	400	140	560	210	840	180	2
RSC 5	400	70	630	105	945	180	2

2.2. Methodology

The concrete mix proportions for M30 grade concrete were prepared according to IS: 10262-2019 [57] guidelines to achieve the target strength. The mix proportions of the developed concrete mixtures are presented in Table 5. After conducting various trial mixes, the optimised mix was obtained with a target strength of 38.26 MPa. Subsequently, the optimised concrete mix was modified by adding copper slag and waste ceramic tiles as fine and coarse aggregates at replacement levels of 50 %, 60 %, 70 %, 80 %, and 90 %.

The cement, M-sand, and coarse aggregate were initially blended under dry conditions, and then half the amount of water superplasticiser was added and mixed thoroughly for approximately 2 to 3 min. Finally, the remaining water superplasticiser was added and mixed for an additional 2 min. The specimens were cast according to IS: 516-2021 [58] for different tests, employing steel moulds, and compacted in two even layers using a table vibrator to ensure external vibration to achieve proper concrete compaction. The specimens were cast for the control (CC) mixtures. For RSC mixes, respective amounts of copper slag and waste ceramic tiles were added in conjunction with fine and coarse aggregates. The specimens were prepared and allowed to cure for approximately 7, 14, and 28 days, and their respective properties were measured. Various tests were planned and conducted according to the standards set by the Bureau of Indian Standards (BIS), American Society for Testing and Material (ASTM), and recommendations of the ACI Committee. Approximately 54 cubes (three specimens for each mix for testing at 7, 14, and 28 d), 54 cylinders (three specimens for each mix for testing at 7, 14, and 28 d), 54 prisms (three specimens for each mix for testing at 7, 14, and 28 d), and 18 slab specimens (three specimens for each mix for testing at 28 d) were cast and tested.

2.3. Testing methods

2.3.1. Slump test

Slump cone tests are generally used to assess the workability of concrete. A slump cone test was conducted to measure the slump values of various concrete mixes: CC, RSC1, RSC2, RSC3, RSC4, and RSC5. The test was conducted according to the IS: 1199-1959 [59] guidelines. The freshly mixed concrete was poured into the oil-applied mould in four layers and a 16 mm-diameter bar was used to tamp each layer 25 times. Once the concrete was poured entirely into the mould, it was gently lifted, and the poured concrete tended to slide. The heights of the concrete slides were also measured.

2.3.2. Density test

The fresh concrete density was determined according to the ASTM C138/C138M standard test method for the density (unit weight), yield, and air content of concrete, using a calibrated cylindrical container of known volume. The concrete was placed in three layers and adequately compacted according to the standard to avoid entrapment of air. The hardened density was later validated using the mass-to-volume ratio of the cubic specimens (150 × 150 × 150 mm) after 28 d of curing.

2.3.3. Compressive strength test

A cubic sample measuring 100 × 100 x 100 mm was cast and used to measure the compressive strength after 7, 14, and 28 d of curing. The test was conducted according to the IS: 516-2021 [58] standards using a universal testing machine (UTM) with a capacity of 1000 kN and minimum count of 1 kN, as illustrated in Figure 4. Three samples were tested to determine the average compressive strength of each concrete mixture.

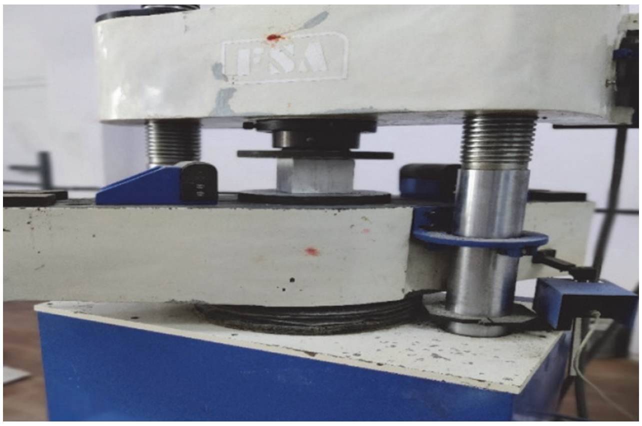

Figure 4. Compressive strength test setup

2.3.4. Split tensile strength test

A cylindrical sample measuring 200 m in height and 100 mm in diameter was cast and used to measure the split tensile strength after 7, 14, and 28 d of curing. The test was conducted according to the guidelines of the IS: 516-2021 [58] standards, utilising a UTM with a capacity of 1000 kN and minimum count of 1 kN, as illustrated in Figure 5. Three samples were tested to determine the average splitting tensile strength of each concrete mixture.

Figure 5. Split tensile strength test setup

2.3.5. Flexural strength test

A prism sample measuring 100 mm × 100 mm × 500 mm was cast and used to measure the flexural strength after 7, 14, and 28 d of curing. Flexural strength (modulus of rupture) tests were conducted according to the specifications of ASTM C78/C78M-21 [60] under four-point loading on a simply supported span of 400 mm using a servo-controlled UTM with a capacity of 1000 kN, as shown in Figure 6. The samples were tested at the deformation rate of 0.1 mm/min. Three samples were tested to determine the average splitting tensile strength of each concrete mixture.

2.3.6. Radiation shielding test

The radiation shielding test was employed to measure the linear attenuation coefficient (μ) of CC and RSC mixes containing copper slag and waste ceramic tiles as aggregates. The concrete slab with a thickness of 15 cm was cast and exposed to gamma rays from a Cesium-137 (Cs-137) source which released gamma rays at an energy level of 0.662 keV. A narrow-beam setup was employed during the experiment to achieve an accurate measurement of radiation attenuation. A NaI (Tl) scintillation detector was placed at a fixed distance of approximately 200 cm from the radiation source, directly in line with the beam path, as illustrated in Figure 7. The concrete slab was exposed to gamma-rays for 60 s. The intensity of radiation passing through the concrete samples was measured using the detector, and the linear attenuation coefficient (μ) was calculated in units of cm^{-1}. The linear attenuation coefficient (μ) defines the probability of gamma-ray interaction with the material for each unit of length. The attenuation coefficient (μ) of the gamma ray was computed to assess the fractional radiation intensity (I) in relation to the source intensity (I_0) across the thickness (x). The linear attenuation coefficient (μ) was evaluated using equation (1).

$$\mu = \frac{\ln\left(\frac{I_0}{I}\right)}{x} \tag{1}$$

Figure 6. Flexural strength test setup.

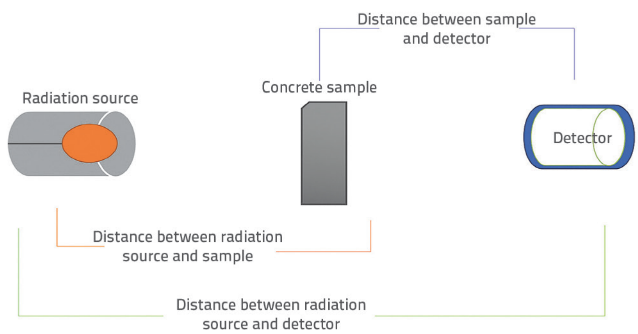

Figure 7. Radiation-shielding test setup

3. Results and discussions

3.1. Density

Figure 8 demonstrates the increase in the density of the CS and RCT aggregate-added concrete compared with the CC mix. The density of the concrete mixes progressively increased as the replacement level of CS and RCT aggregates increased, as observed for the CC to RSC5 mixes. The CC mix containing 100 % natural aggregates exhibited the lowest density of 1611.1 kg/m^3 among the mixes. The RSC1 mix containing 350 kg/m^3 of copper slag as fine aggregate with 525 kg/m^3 of ceramic tiles as coarse aggregate exhibited a density of 1952.3 kg/m^3, which is nearly 21.2 % higher than that of the CC mix. This increase in density is primarily attributed to the higher specific gravity values of CS and RCT compared with those of M-sand and natural coarse aggregate. The same trend was observed across all other modified mixes, that is RSC2, RSC3, RSC4, and RSC5. The maximum increase in density (2350.6 kg/m^3) was observed for RSC5 mix containing 630 kg/m^3 of CS as fine aggregate with 945 kg/m^3 of RCT as coarse aggregate, which is approximately 45.9 % higher than that of CC mix.

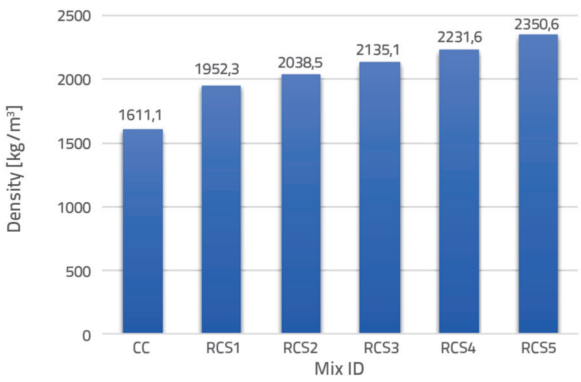

Figure 8. Density of concrete mix

The density of CC (1611.1 kg/m^3) was less than that of mixes with recycled tile aggregate added concrete. As the percentage of recycled tile aggregate increased from RCS1 to RCS5, the density progressively increased, attaining 2350.6 kg/m^3. This enhancement in density can be attributed to the intrinsically dense microstructure of the ceramic tile aggregates, which possess a lower porosity and higher particle hardness than conventional natural coarse aggregates. Furthermore, the denser nature of ceramic slag (CS) and RCT contributed to more efficient particle packing, effectively reducing the interparticle voids within the concrete matrix. The angular shape and rigid structure of the RCT particles promote mechanical interlocking, which not only minimises the void content but also enhances compaction during mixing and placement. These combined effects result in a concrete matrix with a higher unit weight and lower porosity, thereby improving the overall bulk density. This finding aligns with those of Sivakumar et al. [61] and Nepomuceno et al. [62], who reported that the use of RCT as a replacement for coarse aggregates increases the density of concrete compared with conventional concrete (CC). Hosen and Barbulescu [63] also observed that the substantial replacement of ceramic waste aggregates with coarse aggregates in concrete can lead to an increased unit weight because of the reduced void content of the waste aggregate. The ceramic tile aggregates exhibited low porosity, higher compaction, and stronger interlocking, leading to a reduced void content and improved packing density. Therefore, the incorporation of RCT aggregates enhanced the density of the concrete, validating their effectiveness in producing more compact and structurally dense mixes. Such an increase in density not only improves the mechanical properties but also makes the mixes more appropriate for specialised applications such as radiation shielding.

3.2. Slump value

Figure 9 presents the workability properties of the concrete mix containing CS and RCT as fine and coarse aggregates, added at various replacement levels and measured in terms of slump values.

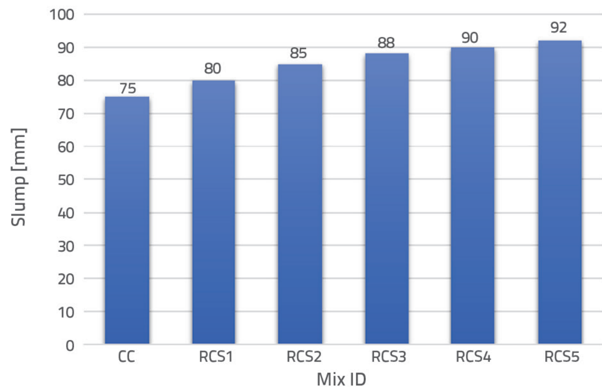

Figure 9. Slump of concrete

The CC mix recorded a slump value of 75 mm, whereas the modified mixes (RCS1, RCS2, RCS3, RCS4, and RCS5) containing CS and RCT as partial replacements for natural fine aggregate and coarse aggregate at various replacement levels of 50 %, 60 %, 70 %, 80 %, and 90 % recorded slump values of 80, 85, 88, 90, and 92 mm, respectively. This indicates that the inclusion of CS and RCT as aggregates in concrete significantly increases the slump value. This increase in the slump can be primarily attributed to the properties of the copper slag. The high specific gravity and smooth glassy surface texture of copper slag minimises the internal friction between particles and acts as a ball-bearing agent in the concrete mix, which facilitates enhanced flow. Furthermore, the lower water absorption rate of copper slag compared with that of M-sand results in more water availability in the mix [64], thereby improving the workability of concrete. Similarly, the angular, irregular, relatively smooth, and less porous surfaces of ceramic tiles result in less water absorption than that of granite stone (coarse aggregate) [65]. This facilitates the concrete mix in retaining more free liquid water, thereby enhancing its flowability. The combined use of copper slag and waste ceramic tiles creates a synergistic effect on the workability of concrete. Although the CS improved the flow characteristics of the mortar matrix, it also counteracted the angularity of the RCTA particles, reducing the overall harshness of the mix. Consequently, the concrete became more cohesive and workable, even at higher replacement levels. This confirms that both CS and RCT are viable alternatives to natural aggregates, capable of enhancing workability and making concrete suitable for applications that require moderate-to-high slump values, such as pumped or precast concrete.

3.3. Compressive strength

Na slici 10. prikazane su tlačne čvrstoće betona s bakrenom The compressive strengths of the concrete containing copper slag and waste ceramic tiles as partial aggregate replacements for 7, 14, and 28 days are presented in Figure 10. At 7 days, the compressive strengths of the RCS1, RCS2, and RCS3 mixes were higher than that of the CC mix; in particular, RCS2 possessed a compressive strength of 27.3 MPa, which is approximately 9.25 % higher than that of the CC mix. This increase in compressive strength was attributed to the effective hydration process caused by the inclusion of CS, which improved the microstructure of the concrete by filling the voids and increasing the density of the mix.

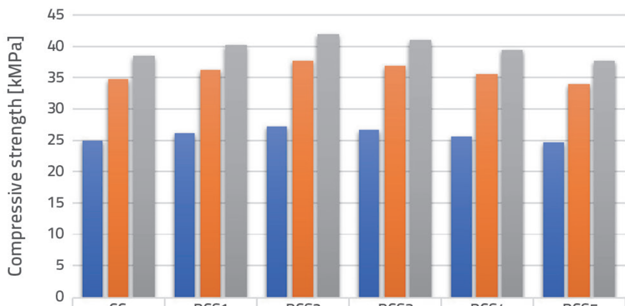

	CC	RCS1	RCS2	RCS3	RCS4	RCS5
7 days	25	26,1	27,3	26,7	25,7	24,6
14 days	34,7	36,2	37,8	36,9	35,6	34
28 days	38,5	40,2	42	41	39,5	37,8

Figure 10. Compressive strength of the concrete

Conversely, RSC5 exhibited a 1.6 % decrease in compressive strength, indicating that a high replacement level might adversely affect early strength development owing to less effective bonding and hydration. At 14 days, the trend continued, with RCS2 exhibiting the highest increment in strength, which was approximately 8.9 % higher than that of the CC mix. The addition of CS and RCT ensured that the materials contributed positively to the concrete matrix without overwhelming the mixture. The RCS5 mix recorded a compressive strength of 37.8 MPa, which is approximately 2 % less than that of the CC mix at 14 days. At 28 days, the trend continued, with RCS2 possessing the highest increment in strength, approximately 9.1 % higher than that of the CC mix, and RCS5 exhibiting a lower compressive strength of approximately 1.8 % less than that of the CC mix. This indicates that, although the addition of CS and RCT exerts positive effects on concrete strength, higher replacement levels (above 60 %) may disrupt the mix composition and lead to a decrease in strength, potentially owing to an increase in porosity or an imbalance between the aggregates and cementitious materials. The findings indicated that replacing fine and coarse aggregates with copper slag and RCT at a 60 % replacement level (RCS2) produced the highest compressive strength. This finding was consistent with the findings of Ouda and Abdelgader [66], who reported that the optimum aggregate replacement level for attaining a better compressive strength of radiation-shielding concrete was 60 %. This optimum performance occurs because the replacement materials aid in improving the hydration, density, and bonding of the concrete. The concrete mix proposed in this study using CS and RCT was found to be superior in terms of compressive strength than those in existing studies. Badarloo et al. [67] developed RSC using barite aggregates and observed that the replacement of barite aggregate decreased the compressive strength by 20.82 to 27.52 %. Najimi et al. [68] and Mirhossein et al. [69] found that the compressive strength of concrete with copper slag decreased as the amount of copper slag in the aggregates increased, particularly when added at a 30 % replacement level. However, this study demonstrated a 9.1 % improvement in compressive strength with the combined addition of 60 % CS and RCT as aggregates.

3.4. Split tensile strength

The split tensile strengths of the concrete containing CS and RCTA as partial aggregate replacements for 7, 14, and 28 days are presented in Figure 11.

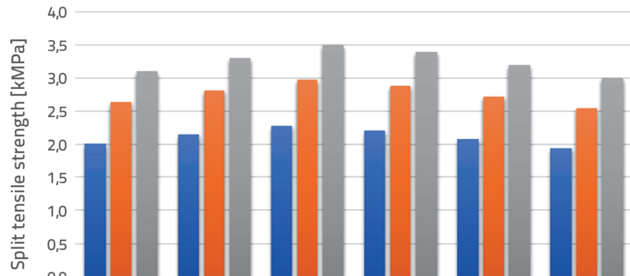

	CC	RCS1	RCS2	RCS3	RCS4	RCS5
7 days	2,02	2,15	2,28	2,21	2,08	1,95
14 days	2,64	2,81	2,98	2,89	2,72	2,55
28 days	3,1	3,3	3,5	3,4	3,2	3

Figure 11. Split tensile strength of the concrete

At 7 days, the split tensile strengths of the concrete mixes containing 50 %, 60 %, 70 %, and 80 % CS and RCT were 6.44 %, 12.87 %, 9.41 %, and 2.97 % higher, respectively, than those of the CC mix, as observed for the RSC1, RSC2, RSC3, and RSC4 mixes. At 14 days, the split tensile strengths of the concrete mixes containing 50 %, 60 %, 70 %, and 80 % CS and RCTA were 6.44 %, 12.88 %, 9.47 %, and 3.03 % higher, respectively, than those of the CC mix, as observed for the RSC1, RSC2, RSC3, and RSC4 mixesAt 28 days, the split tensile strengths of the concrete mixes containing 50 %, 60 %, 70 %, and 80 % CS and RCT were 6.45 %, 12.9 %, 9.68 %, and 3.23 % higher, respectively, than those of the CC mix, as observed for mixes RSC1, RSC2, RSC3, and RSC4. The findings indicated that incorporating copper slag and waste ceramic tiles improved the split tensile strength to a replacement rate of 60-80 %. This improvement is attributed to the increased packing density, filler properties, and pozzolanic activity of the copper slag [70, 71], which enhances the interfacial transition zone and distribution of tensile loads. Waste ceramic tiles, with their rigid and angular structure, potentially enhance mechanical interlocking, thereby increasing strength [72-74]. However, at higher replacement levels (particularly at 90 % in RCS5), a decrease in strength was observed, likely owing to the excessive angularity, increased voids, and weaker adhesion between the paste and aggregates, which reduced the tensile resistance of the concrete matrix. This finding aligns with the those of Ouda and Abdelgader [66], who indicated that the tensile strength increased by 1.90, 8.25 %, and 11.74 % when natural aggregate was replaced with limestone aggregate at rates of 20 %, 40 %, and 60 %, respectively. However, in this study, a maximum improvement of 12.95 was achieved for a 60 % aggregate replacement level using CS and RCT.

3.5. Flexural strength

The flexural strengths of the concrete containing CS and RCT as partial aggregate replacements for 7, 14, and 28 days are presented in Figure 12.

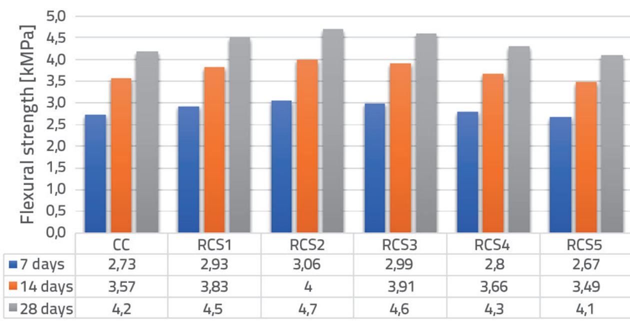

Figure 12. Flexural strength of the concrete

At 7 days, the modified mixes, such as RSC1, RSC2, RSC3, and RSC4, demonstrated higher flexural strengths than that of the CC mix, which exhibited a strength of 2.73 MPa. The RSC1, RSC2, RSC3, and RSC4 mixes exhibited flexural strengths approximately 7.33 %, 12.09 %, 9.52 %, and 2.56 % higher than that of the CC mix, respectively. RSC2 mix, with 60 % CS and RCT, exhibited the highest improvement in flexural strength, indicating that a 60 % replacement level offers optimal particle packing and enhanced early age strength attributable to the filler and pozzolanic properties of CS [70, 71]. However, the RCS5 mix exhibited a marginal decrease of approximately 2.20 % in flexural strength, indicating that a high replacement level (90 %) may weaken the early age strength owing to poor bonding and increased porosity. At 14 days, the same trend was observed; the modified mixes RSC1, RSC2, RSC3, and RSC4 demonstrated higher flexural strengths than that of the CC mix, which exhibited a flexural strength of 3.57 MPa. The flexural strengths of the RSC1, RSC2, RSC3, and RSC4 mixes were 7.28 %, 12.03 %, 9.53 %, and 2.2 % higher than that of the CC mix, respectively. The flexural strength of the RSC5 mix decreased by 2.24 % compared with that of the control mix owing to the weakened cement matrix and poor aggregate bond resulting from excessive replacement. At 28 days, the same trend was observed; the modified mixes, such as RSC1, RSC2, RSC3, and RSC4, demonstrated a higher flexural strength than that of the CC mix. The RSC2 mix achieved a flexural strength of 4.70 MPa, reflecting an 11.90 % increase over the control mix (4.20 MPa). The RSC3 and RCS1 mixes exhibited improvements of 9.52 % and 7.14 % over the control mix. RSC4 showed a modest strength gain of 2.38 %, whereas RCS5 underperformed, with a 2.38 % decrease over the CC mix. The consistent peak performance of RCS2 across all the curing days confirms that a 60 % replacement level achieves a balance between strength and sustainability. Conversely, a decrease in RSC5 indicates that the excessive use of CS and RCT may impair concrete quality owing to increased angularity, poor workability, and weakened matrix integrity [75]. Therefore, it was concluded that the use of CC and RCT as aggregates in concrete significantly increased the flexural strength of concrete. Similar findings were reported by Shahid et al. [76] who used iron-cutting waste as an aggregate in concrete.

3.6. Attenuation coefficient (μ)

Koeficijent prigušenja (μ) temeljni je pokazatelj učinkovitosti betonskog materijala u zaštiti od zračenja. Na slici 13. prikazani su koeficijenti prigušenja za betone s djelomičnom zamjenom agregata CS-om i RCT-om.

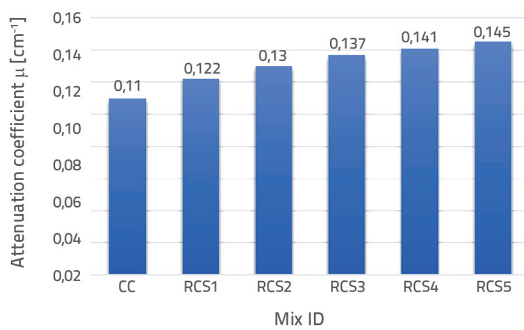

Figure 13. Attenuation coefficient of concrete mix

The attenuation coefficient (μ) serves as a fundamental metric to assess the efficiency of concrete material when used for radiation against shielding. Figure 13 presents the attenuation coefficients for concrete containing CS and RCT as partial aggregate replacement. The results of the radiation shielding test indicated that as the replacement levels of CS and RCT in the concrete mix increased, the attenuation coefficient increased, demonstrating an improved ability to attenuate gamma radiation. The CC mix exhibited an attenuation coefficient of 0.110 cm^{-1}. With the inclusion of copper slag and waste ceramic tiles, the attenuation coefficient increased progressively. The RSC1, RSC2, RSC3, RSC4 and RSC5 mix with 50 %, 60 %, 70 %, 80 % and 90 % of CS and RCT exhibited an attenuation coefficient of 0.122 cm^{-1}, 0.130 cm^{-1}, 0.137, 0.141 and 0.145 cm^{-1}, which are approximately 10.9 %, 17.27 %, 24.55 %, 28.18 % and 31.82 %, respectively, higher than that of the CC mix. This indicates that incorporating CS and RCT, which possess different densities and atomic structures than natural aggregates, results in an enhancement in shielding. This is likely owing to the optimal balance between the physical properties of the CS and RCT. The higher attenuation coefficient observed with increased replacement levels indicates that CS and RCT not only increase the mechanical properties of concrete but also enhance its capacity to block or reduce gamma radiation penetration. This finding is consistent with the findings of Azeez et al. [77], who reported that the linear attenuation coefficients increased as the waste material content in the concrete increased. Azeez et al. [78] noted a significant enhancement of 20 to 25 % in the attenuation performance achieved for concrete containing iron waste fillings at various loading rates (5 to 30 %). Ibrahim et al. [79] reported that the replacement of natural aggregate with 30 % haematite and 30 % iron slag in concrete enhancement of 9.32 % to 1.9 % in attenuation performance. However, a 28.18 % improvement in attenuation performance was achieved using CS and RCT in concrete. The concrete mix that included copper slag and waste ceramic tiles exhibited improved radiation-shielding properties with superior mechanical properties, as observed for RCS2 (60 % replacement), delivering the highest performance in terms of attenuation. This RCS2 mix composition is most suitable for applications where radiation protection is essential, such as the construction of nuclear laboratories, medical radiology rooms, and X-ray shielding.

3.7. Correlation between attenuation coefficient and density

Figure 14 illustrates a strong positive linear correlation between the attenuation coefficient (cm^{-1}) and density (kg/m^3) of the concrete mix that include various proportions of CS and RCT.

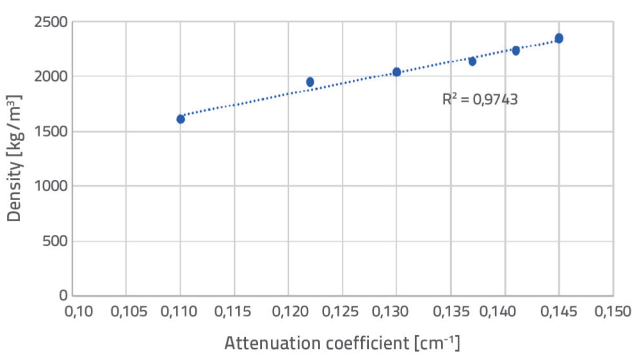

Figure 14. Correlation between the attenuation coefficient and density

The coefficient of determination (R^2 = 0.9743) indicated a significantly high correlation, indicating that the gamma radiation shielding properties of concrete were strongly related to its density. The density of the concrete mix increased from 1611 kg/m^3 to 2350.6 kg/m^3 with the inclusion of CS and RCT as fine and coarse aggregates, respectively, at the 90 % replacement level. Correspondingly, the attenuation coefficient increases with density, indicating that denser concrete mixes are more efficient at absorbing or attenuating gamma radiation. Similar findings have been reported in previous studies [80-83].

This trend has a scientifically basis because denser materials typically possess more mass per unit volume, offering a higher atomic number of atomic nuclei with which gamma rays can interact. Copper slag, with its high specific gravity and high metallic content, contributes significantly to the shielding effect. Similarly, waste ceramic tiles contribute to the compactness and density, thereby improving the radiation-attenuation properties of concrete. Therefore, concrete mixes modified with CS and RCT provide not only sustainable material alternatives but also improve functional properties such as radiation shielding, making them appropriate for application in nuclear, medical, and industrial radiation environments.

4. Conclusions

This study developed gamma radiation-shielding concrete using CS and RCT as aggregates. The primary conclusions drawn from this study are as follows.

- The incorporation of CS and RCT into concrete significantly improved its radiation-shielding properties while maintaining or improving its mechanical properties.
- The RSC2 mix showed the optimal combination of strength and gamma radiation attenuation properties while also achieving flexural strength of 4.70 MPa in conjunction with split tensile strength 12.9 % higher than that of the CC and an attenuation coefficient of 0.130 cm^{-1}, which provided 17.27 % higher radiation shielding in terms of attenuation coefficient compared with the CC.
- The higher replacement levels of fine and coarse aggregates with CS and RCT further increased the attenuation coefficient to a maximum of 0.145 cm^{-1}, representing a 31.82 % improvement. However, replacement levels exceeding 60 %, as observed for RSC3 and RSC5, resulted in a marginal reduction in mechanical strength.
- The RSC5 mix showed maximum density of 2350.6 kg/m^3 among all mixes and exhibited strong correlation between density values (R^2 = 0.9743) and shielding effectiveness results.
- The findings demonstrate the effectiveness of using CS and RCT as aggregates at a replacement level of 60 % to develop a durable and effective gamma radiation shielding concrete suitable for use in nuclear laboratories, medical radiology rooms, and X-ray shielding applications.
- The RSC2 mix offers optimal performance properties and economic advantages for generating a concrete material which strengthens and protects against radiation, while maintaining structural integrity.

A limitation of this study is the absence of direct porosity measurements, a factor that significantly influences density, water absorption, strength, and durability of concrete. Future research should incorporate direct testing of porosity to enable a more comprehensive assessment of material performance.

REFERENCES

[1] Oluwasola, E.A., Afolayan, A., Ipindola, O.O., Popoola, M.O., Oginni, A.O.: Effect of aggregate shapes on the properties of concrete, LAUTECH Journal of Civil and Environmental Studies, 5 (2020), pp. 1-10.

[2] Hemalatha, T., Sangoju, B., Muthuramalingam, G.: A study on copper slag as fine aggregate in improving the electrical conductivity of cement mortar, Sādhanā, 47 (2020), p. 141.

[3] Akbulut, H., Gürer, C.: Use of aggregates produced from marble quarry waste in asphalt pavements, Building and environment, 42 (2007), pp. 1921-1930.

[4] Aliabdo, A.A., Abd-Elmoaty, A.E.M., Hassan, H.H.: Utilization of crushed clay brick in concrete industry, Alexandria Engineering Journal, 53 (2014), pp. 151-168.

[5] Tripathi, E., Patowari, P.K., Pati, S.: Assessment of mixing performance in a spiral micromixer with different inlet path configurations. Sādhanā, 47 (2022), p. 240.

[6] Wu, K., Chen, F., Chen, C., Lin, S., Nan, Y.: Study of basic mechanical properties of recycled concrete with various recycled coarse aggregate mixes, Građevinar, 75 (2023) 1, pp. 1-12, https://doi.org/10.14256/JCE.2244.2017

[7] Shi, C., Meyer, C., Behnood, A.: Utilization of copper slag in cement and concrete, Resources, Conservation and Recycling, 52 (2008), pp. 1115-1120.

[8] Brindha, D., Baskaran, T., Nagan, S.: Assessment of corrosion and durability characteristics of copper slag admixed concrete, International Journal of Civil and Structural Engineering, 1 (2010), p. 192.

[9] Lye, C.Q., Koh, S.K., Mangabhai, R., Dhir, R.K.: Use of copper slag and washed copper slag as sand in concrete: a state-of-the-art review, Magazine of Concrete Research, 67 (2015), pp. 665-679.

[10] Soni, M.M., Mangroliya, J.R.: Performance of copper slag on strength as partial replacement of fine aggregate in concrete, International Journal of Engineering Research and Technology, 7 (2015), p. 347.

[11] Silva, Y.F., Burbano-Garcia, C., Araya-Letelier, G., Gonzalez, M.: Short-and long-term experimental performance of concrete with copper slag: Mechanical and physical properties assessment, Case Studies in Construction Materials, 20 (2024), p. e03302.

[12] Al-Jabri, K.S., Al-Saidy, A.H., Taha, R.: Effect of copper slag as a fine aggregate on the properties of cement mortars and concrete, Construction and Building Materials, 25 (2011), pp. 933-938.

[13] Gupta, N., Siddique, R.: Durability characteristics of self-compacting concrete made with copper slag, Construction and Building Materials, 247 (2020), p. 118580.

[14] Divya, S., Praveenkumar, S.: An integrated evaluation of graphene-based concrete mixture with copper slag and quarry dust using response surface methodology, Journal of Building Engineering, 86 (2024), p. 108876

[15] Sanchez, E., García-Ten, J., Sanz, V., Moreno, A.: Porcelain tile: almost 30 years of steady scientific-technological evolution, Ceramics International, 36 (2010), pp. 831-845.

[16] Baraldi, L.: World Production and Consumption of Ceramic Tiles, Ceramic World, 41 (2021), pp. 26-40.

[17] Pacheco-Torgal, F., Jalali, S.: Reusing ceramic wastes in concrete, Construction and Building Materials, 24 (2010), pp. 832-838.

[18] Tawfeeq, W.M., Alsaidi, M., Al-Kamzari, A., Al-Shibli, M., Al-Mamari, Z.: Using Crushed Tiles as Coarse Aggregate in Concrete Mix, In 3rd International Conference on Civil, Environment and Waste Management (2016), pp. 12-14.

[19] Al-Labban, S.N.Y., Abdullah, F.A., Karagoly, Y.H., Shubber, M.S., Hasan, S.A., Jabal, Q.A.: Waste aggregate concrete properties using waste tiles as coarse aggregate and modified with PC superplasticizer, Open Engineering, 12 (2022), pp. 1089-1096.

[20] Keshavarz, Z., Mostofinejad, D.: Porcelain and red ceramic wastes used as replacements for coarse aggregate in concrete, Construction and Building Materials, 195 (2019), pp. 218-230.

[21] Tawfik, T.A., Sičáková, A., Kuzielová, E., Kušnír, Š., Eštoková, A., Bálintová, M., Junáková, N.: Sustainable reuse of waste ceramic tiles powder and waste brick powder as a replacement for cement on green high strength concrete properties, Innovative Infrastructure Solutions, 9 (2024), p. 166.

[22] Priya, S.A., Ray, S., Haque, M., Mita, A.F., Hossain, Z.: Experimental and numerical investigation of the properties of concrete with ceramic tile waste and stone dust as substitutes for natural aggregates, Discover Civil Engineering, 1 (2024), p. 120.

[23] Baričević, A., Kovač, D., Didulica, K.: Construction of a new day hospital in Zadar using recycled aggregate concrete, Građevinar, 73 (2021) 8, pp. 833-844, https://doi.org/10.14256/JCE.3233.2021.

[24] Lawrence, D.J., Feldman, W.C., Gold, R.E., Goldsten, J.O., McNutt, R.L.: The neutron, gamma-ray, X-ray spectrometer (NGXS): A compact instrument for making combined measurements of neutrons, gamma-rays, and X-rays, Acta Astronautica, 93 (2014), pp. 524-529.

[25] Zayed, A.M., Masoud, M.A., Rashad, A.M., El-Khayatt, A.M., Sakr, K., Kansouh, W.A., Shahien, M.G.: Influence of heavyweight aggregates on the physico-mechanical and radiation attenuation properties of serpentine-based concrete, Construction and Building Materials, 260 (2020), p. 120473.

[26] Portugal-Pereira, J., Ferreira, P., Cunha, J., Szklo, A., Schaeffer, R., Araújo, M.: Better late than never, but never late is better: Risk Assessment of Nuclear Power Construction Projects, Energy Policy, 120 (2018), pp. 158-166.

[27] Jin, T., Kim, J.: What is better for mitigating carbon emissions-Renewable energy or nuclear energy? A panel data analysis, Renewable and Sustainable Energy Reviews, 91 (2018), pp. 464-471.

[28] Mahmood, N., Wang, Z., Zhang, B.: The role of nuclear energy in the correction of environmental pollution: Evidence from Pakistan, Nuclear Engineering and Technology, 52 (2020), pp. 1327-1333.

[29] Ustabas, I., Demirci, M., Baltas, H., Demir, Y., Erdogdu, S., Kurt, Z., Cakmak, T.: Mechanical and radiation attenuation properties of conventional and heavy concrete with diverse aggregate and water/cement ratios, Građevinar, 74 (2022) 8, pp. 635-645, https://doi.org/10.14256/JCE.3382.2021.

[30] Al-Tersawy, S.H., El-Sadany, R.A., Sallam, H.E.M.: Experimental gamma-ray attenuation and theoretical optimization of barite concrete mixtures with nanomaterials against neutrons and gamma rays, Construction and Building Materials, 289 (2021), p. 123190.

[31] Aygün, B., Şakar, E., Agar, O., Sayyed, M. I., Karabulut, A., Singh, V. P.: Development of new heavy concretes containing chrome-ore for nuclear radiation shielding applications, Progress in Nuclear Energy, 133 (2021), p 103645.

[32] AbuAlRoos, N.J., Amin, N.A.B., Zainon, R.: Conventional and new lead-free radiation shielding materials for radiation protection in nuclear medicine: A review, Radiation Physics and Chemistry, 165 (2019), p. 108439.

[33] Zhao, H., Jiang, K., Yang, R., Tang, Y., Liu, J.: Experimental and theoretical analysis on coupled effect of hydration, temperature and humidity in early-age cement-based materials, International Journal of Heat and Mass Transfer, 146 (2020), p. 118784.

[34] Liu, J., Tian, Q., Wang, Y., Li, H., Xu, W.: Evaluation method and mitigation strategies for shrinkage cracking of modern concrete, Engineering, 7 (2021), pp. 348-357.

[35] Akkurt, İ., Başyiğit, C., Akkaş, A., Kılınçarslan, Ş., Mavi, B., Günoğlu, K.: Determination of some heavyweight aggregate half value layer thickness used for radiation shielding, Acta Physica Polonica A, 121 (2012), pp. 138-140.

[36] Monte, F.L., Gambarova, P.G.: Thermomechanical behaviour of baritic concrete exposed to high temperature, Cement and Concrete Composites, 53 (2014), pp. 305-315.

[37] González-Ortega, M.A., Cavalaro, S.H.P., Aguado, A.: Influence of barite aggregate friability on mixing process and mechanical properties of concrete. Construction and Building Materials, 74 (2015), pp. 169-175.

[38] Ouda, A.S., Abdel-Gawwad, H.A.: The effect of replacing sand by iron slag on physical, mechanical and radiological properties of cement mortar. HBRC Journal, 13 (2017) 3, 255-261.

[39] Cullu, M., Bakırhan, E.: Investigation of radiation absorption coefficients of lead-zinc mine waste rock mixed heavy concrete at 662-1460 keV energy range, Construction and Building Materials, 173 (2018), pp. 17-27.

[40] Papachristoforou, M., Papayianni, I.: Radiation shielding and mechanical properties of steel fiber reinforced concrete (SFRC) produced with EAF slag aggregates, Radiation Physics and Chemistry, 149 (2018), pp. 26-32.

[41] Dezhampanah, S., Nikbin, I.M., Mehdipour, S., Mohebbi, R., Moghadam, H.: Fiber-reinforced concrete containing nano-TiO2 as a new gamma-ray radiation shielding materials, Journal of Building Engineering, 44 (2021), pp. 102542.

[42] Rawat, G., Gandhi, S., Murthy, Y.I.: A critical assessment on the effect of nano-titanium dioxide on the properties of concrete, Građevinar, 74 (2022) 7, pp. 553-560.

[43] Abo-El-Enein, S.A., El-Hosiny, F.I., El-Gamal, S.M.A., Amin, M.S., Ramadan, M.: Gamma radiation shielding, fire resistance and physicochemical characteristics of Portland cement pastes modified with synthesized Fe2O3 and ZnO nanoparticles, Construction and Building Materials, 173 (2018), pp. 687-706.

[44] Ling, T.C., Poon, C.S.: Feasible use of recycled CRT funnel glass as heavyweight fine aggregate in barite concrete, Journal of Cleaner Production, 33 (2012), pp. 42-49.

[45] Alwaeli, M.: Investigation of gamma radiation shielding and compressive strength properties of concrete containing scale and granulated lead-zinc slag wastes, Journal of Cleaner Production, 166 (2017), pp. 157-162.

[46] Baalamurugan, J., Kumar, V.G., Chandrasekaran, S., Balasundar, S., Venkatraman, B., Padmapriya, R., Raja, V. B.: Utilization of induction furnace steel slag in concrete as coarse aggregate for gamma radiation shielding, Journal of Hazardous Materials, 369 (2019), pp. 561-568.

[47] IS: 12269-1987, Ordinary Portland Cement, 53 grades - Specifications.

[48] IS: 383-1970, Specification for coarse and fine aggregates from natural sources for concrete.

[49] IS: 456-2000, Plain and reinforced concrete, Code of Practice.

[50] ASTM C 494-13, Standard specifications for chemical admixtures for concrete.

[51] Hwang, C.L., Laiw, J.C.: Properties of concrete using copper slag as a substitute for fine aggregate, Special Publication, 114 (1989), pp. 1677-1696.

[52] Madheswaran, C.K., Ambily, P.S., Dattatreya, J.K., Rajamane, N.P.: Studies on use of copper slag as replacement material for river sand in building constructions, Journal of the Institution of Engineers (India): Series A, 95 (2014), pp. 169-177.

[53] Raman, J.V.M., Rajesh, R., Velswaran, P.S.: Study on strength of high-performance concrete by partial replacement of fine aggregate by copper slag, International Journal of Applied Engineering Research, 14 (2019), pp. 2795-2798

[54] Maharishi, A., Singh, S.P., Gupta, L.K.: Strength and durability studies on slag cement concrete made with copper slag as fine aggregates, Materials Today: Proceedings, 38 (2021), pp. 2639-2648.

[55] IS: 2386 (Part 3)-1963, Methods of test for aggregates for concrete.

[56] IS: 2386 (Part 1)- 1963, Methods of test for aggregates for concrete.

[57] IS: 10262-2019, Concrete mix design.

[58] IS: 516-2021, Hardened concrete methods of test part 1 testing of strength of hardened concrete section-1 compressive, flexural, and split tensile strength.

[59] IS: 1199-1959, Methods of sampling and analysis of concrete.

[61] ASTM C78/C78M-21, Standard test method for flexural strength of concrete (using a simple beam with third-point loading)

[62] Sivakumar, A., Srividhya, S., Sathiyamoorthy, V., Seenivasan, M., Subbarayan, M.R.: Impact of waste ceramic tiles as partial replacement of fine and coarse aggregate in concrete, Materials Today: Proceedings, 61 (2022), pp. 224-231.

[63] Nepomuceno, M.C., Isidoro, R.A., Catarino, J.P.: Mechanical performance evaluation of concrete made with recycled ceramic coarse aggregates from industrial brick waste, Construction and Building Materials, 165 (2018), pp. 284-294.

[64] Hosen, K., Bărbulescu, A.: Sustainable concrete using ceramic tile waste as a substitute for brick aggregate, Materials, 18 (2025), p. 3093.

[65] Jin, Q., Chen, L.: A review of the influence of copper slag on the properties of cement-based materials, Materials, 15 (2022), p. 8594.

[66] Anderson, D.J., Smith, S.T., Au, F.T.: Mechanical properties of concrete utilising waste ceramic as coarse aggregate, Construction and Building Materials, 117 (2016), pp. 20-28.

[67] Ouda, A.S., Abdelgader, H.S.: Assessing the physical, mechanical properties, and γ-ray attenuation of heavy density concrete for radiation shielding purposes, Geosystem Engineering, 22 (2019), pp. 72-80.

[68] Badarloo, B., Lehner, P., Bakhtiari Doost, R.: Mechanical properties and gamma radiation transmission rate of heavyweight concrete containing barite aggregates, Materials, 15 (2022), p. 2173.

[69] Najimi, M., Sobhani, J., Pourkhorshidi, A.R.: Durability of copper slag contained concrete exposed to sulfate attack, Construction and Building materials, 25 (2011), pp. 1895-1905.

[70] Mirhosseini, S.R., Fadaee, M., Tabatabaei, R., Fadaee, M.J.: Mechanical properties of concrete with Sarcheshmeh mineral complex copper slag as a part of cementitious materials, Construction and Building Materials, 134 (2017), pp. 44-49.

[71] Casagrande, C.A., Santos, D.D.D., Jochem, L.F., Nóbrega, A.C.D.: Evaluation of copper slag as aggregate addition on properties of cementitious matrix, Matéria (Rio de Janeiro), 25 (2020), p. e-12889.

[72] Moura, W.A., Gonçalves, J.P., Lima, M.B.L.: Copper slag waste as a supplementary cementing material to concrete, Journal of Materials Science, 42 (2007), pp. 2226-2230

[73] Cabalar, A.F., Hassan, D.I., Abdulnafaa, M.D.: Use of waste ceramic tiles for road pavement subgrade. Road Materials and Pavement Design, 18 (2017), pp. 882--96.

[74] Zhang, P., Zhang, P., Wu, J., Guo, Z., Zhang, Y., Zheng, Y.: Mechanical properties and durability of sustainable concrete manufactured using ceramic waste: A review, Journal of Renewable Materials, 11 (2023), pp. 1-18.

[75] Nasare, R., Shah, V., Joshi, T., Dave, U., Ghaffar, S.H.: Exploring sustainable utilization of ceramic waste in heat-resistant concrete: A comprehensive review, International Journal of Applied Ceramic Technology, 22 (2025), p. e15021

[76] Arif, R., Javed, M.F., Asghar, R., Iqtidar, A., Ahmed, B., Alyousef, R., Khan, M.A.: A scientometric review on the utilization of copper slag as a substitute constituent of ordinary Portland cement concrete, Reviews on Advanced Materials Science, 64 (2025), p. 20240082.

[77] Shahid, S., Amjad, R., Ali, S.: Evaluation of mechanical and shielding properties of normal weight concrete by incorporating iron cutting waste (ICW), Iranian Journal of Science and Technology, Transactions of Civil Engineering, 46 (2022), pp. 117-132.

[78] Azeez, A.B., Mohammed, K.S., Al Bakri, A.M., Hasan, H.I., Abdulkareem, O.A.: Radiation shielding characteristics of concretes incorporates different particle sizes of various waste materials, Advanced Materials Research, 925 (2014), pp. 190-194.

[79] Azeez, A.B., Mohammed, K.S., Abdullah, M.M.A.B., Hussin, K., Sandu, A.V., Razak, R.A.: The effect of various waste materials' content on the attenuation level of anti-radiation shielding concrete, Materials, 6 (2013), pp. 4836-4846.

[80] Ibrahim, A.M., Mohamed, A.R., El-Khatib, A.M., Alabsy, M.T., Elsalamawy, M.: Effect of hematite and iron slag as aggregate replacement on thermal, mechanical and gamma-radiation shielding properties of concrete, Construction and Building Materials, 310 (2021), p. 125225.

[81] Akyuz, S.: Heavyweight concrete with barite aggregate for protecting structures against gamma rays, ITU J, 35 (1977), pp. 59-69.

[82] González-Ortega, M.A., Segura, I., Cavalaro, S.H.P., Toralles-Carbonari, B., Aguado, A., Andrello, A.C.: Radiological protection and mechanical properties of concretes with EAF steel slags Construction and Building Materials, 51 (2014), 432-438.

[83] Ouda, A.S.: Development of high-performance heavy density concrete using different aggregates for gamma-ray shielding, HBRC Journal, 11 (2015), pp. 328-338.

[84] Ozen, S., Şengül, C., Erenoğlu, T., Çolak, Ü., Reyhancan, I.A., Taşdemir, M.A.: Properties of heavyweight concrete for structural and radiation shielding purposes, Arabian Journal for Science and Engineering, 41 (2016), pp. 1573-1584.